

The conductivity of thin wires in a magnetic field

By R. G. CHAMBERS, *Royal Society Mond Laboratory, University of Cambridge*

(Communicated by Sir Lawrence Bragg, F.R.S.—Received 18 February 1950—
Revised 20 March 1950)

A thin film or wire of metal has a lower electrical conductivity than the bulk material if the thickness is comparable with or smaller than the electronic mean free path. Previous workers have obtained expressions for the magnitude of the effect by integrating the Boltzmann equation and imposing the appropriate boundary conditions. The problem is re-examined from a kinetic theory standpoint, and it is shown that the same expressions are obtained by this method, usually rather more simply, while the physical picture is considerably clarified. The method is applied to an evaluation of the conductivity of a thin wire with a magnetic field along the axis, and it is found that the resistivity should decrease as the magnetic field is increased; it should be possible to derive the mean free path and velocity of the conduction electrons by comparison of theory and experiment. The theory has been confirmed by experimental measurements on sodium; estimates of electronic velocity and mean free path are obtained which are in fair agreement with the values given by the free-electron theory.

INTRODUCTION

1. It has been realized for many years that the apparent resistivity of a conductor will be increased when its linear dimensions become comparable with, or smaller than, the electronic mean free path, and that from the magnitude of the effect the mean free path may be estimated. Thomson (1901) first gave an approximate expression for the increase in resistivity of a thin film; another approximation was given by Lovell (1936), and the exact solution for a free-electron metal was given by Fuchs (1938). For thin wires a very simple approximation due to Nordheim (1934) has been used by Eucken & Förster (1934) and succeeding workers. Interest in these problems has recently been revived by the work of Andrew (1949) on thin films of tin and thin wires of mercury, and particularly of MacDonald (1949), who showed that for a thin wire of sodium the resistivity actually decreased in a magnetic field, instead of increasing as for the bulk metal, because of the lengthening of the effective mean free path caused by the spiral motion of the electrons in the magnetic field. This opens up the possibility of determining not only the electronic mean free path, but also the momentum of the electrons at the surface of the Fermi distribution, since this determines the radius of the electronic orbits in a given field.

2. Sondheimer (1949) and MacDonald & Sarginson (1949) have recently given solutions for the variation in resistivity of a thin film with a magnetic field applied at right angles to the electric field, and either at right angles to or in the plane of the film. Experimentally, however, it is difficult to make reliable measurements on thin films, particularly on evaporated films, owing to the various possible disturbing effects (Reinders & Hamburger 1931; Lovell 1936–8), and experiments on thin wires may be easier to carry out. Dingle (1950) has recently given the exact theory of the increase in resistivity of a thin wire in the absence of a magnetic field, and MacDonald & Sarginson (in course of publication) have analyzed the case of a wire of rectangular,

and in particular of square, cross-section, and obtained results in the latter case similar to Dingle's.

The aims of the present paper are twofold: first, to show that an exact solution of these small-conductor problems can often be obtained very simply by kinetic theory arguments, without solving the Boltzmann equation *ab initio*, and secondly, to apply this method to the problem of a thin wire with a magnetic field along the axis. Experimental results are given which agree with the theoretical predictions.

THE KINETIC THEORY SOLUTION OF THIN-CONDUCTOR PROBLEMS

The case $H = 0, \epsilon = 0$

3. We consider first the case $H = 0, \epsilon = 0$, where ϵ is defined, following Fuchs, as the proportion of electrons which are specularly reflected at the surface of the metal, retaining their drift velocities, while the remainder $(1 - \epsilon)$ are diffusely reflected, with loss of drift velocity. The representation of the reflexion at the surface by a single parameter ϵ is, of course, very much of an idealization, just as is the representation of the scattering probability in the bulk metal by the single parameter l . Consider a point O in the metal and consider electrons passing through it in the direction \mathbf{OP} where P is on the surface of the metal. Then assuming that the probability of an electron travelling a distance greater than x is $e^{-x/l}$, for $x < OP$, but that electrons which arrive at P will certainly collide there (so that $\epsilon = 0$), it is easily shown that the mean distance travelled by an electron without collision after passing through the point O is

$$l_1 = l(1 - e^{-OP/l}), \quad (1)$$

and it can similarly be shown that, for electrons travelling in the opposite direction \mathbf{PO} , the mean distance travelled without collision before reaching O is also given by equation (1).

In the presence of an electric field E_z in the z direction, these electrons will therefore have acquired a mean drift velocity

$$\Delta v_z = \frac{eE_z}{mv} l(1 - e^{-OP/l}) = \frac{eE_z \tau}{m} (1 - e^{-OP/l}), \quad (2)$$

where v is the speed $|\mathbf{v}|$ of the electrons. We assume, in the usual way, that $N(\mathbf{v}, \mathbf{r})$, the electron density function, is only slightly different from $N_0(\mathbf{v}, \mathbf{r})$, and that $N_0(\mathbf{v}, \mathbf{r}) = N_0(|\mathbf{v}|)$ only. It is tempting at this point to suppose that the mean drift current density at the point O , due to electrons travelling in the direction \mathbf{PO} , is given simply by $eN_0(\mathbf{v}) \Delta v_z$, and that the total drift current density at O is given by

$$j(O) = \frac{e^2 E_z \tau}{m} \int_0^\infty N_0(v) v^2 dv \int_0^{2\pi} d\phi \int_0^\pi d\theta \sin \theta (1 - e^{-OP/l}), \quad (3)$$

where the distance OP is to be expressed as a function of the angles θ and ϕ which define the direction of the vector \mathbf{PO} , θ being the angle between the direction \mathbf{PO} and the z axis, and ϕ the azimuthal angle around the z axis. In fact, however, this approach neglects the fact that $N_0(|\mathbf{v}|)$ is not the same as $N_0(|\mathbf{v} + \Delta v_z|)$; what

determines the drift current is the change n in the number of electrons travelling in the direction **PO** with velocity v due to the presence of the field. This is given by

$$n(\mathbf{PO}) = \frac{\partial N_0}{\partial v_z} \Delta v_z = \frac{eE_z \tau}{m} \frac{\partial N_0}{\partial v_z} (1 - e^{-OP/l}), \quad (4)$$

and the total drift current is given by

$$\begin{aligned} j(O) &= \int_0^\infty v^2 dv \int_0^{2\pi} d\phi \int_0^\pi d\theta \sin \theta ev_z n(\mathbf{PO}) \\ &= \frac{e^2 E_z \tau}{m} \int_0^\infty v^2 dv \int_0^{2\pi} d\phi \int_0^\pi d\theta \sin \theta v_z \frac{\partial N_0}{\partial v_z} (1 - e^{-OP/l}) \\ &= \frac{e^2 E_z \tau}{m} \int_0^\infty v^3 \frac{\partial N_0}{\partial v} dv \int_0^{2\pi} d\phi \int_0^\pi d\theta \sin \theta \cos^2 \theta (1 - e^{-OP/l}) \end{aligned} \quad (5)$$

When the distance OP is independent of (θ, ϕ) , the expression (5) reduces to expression (3), but not otherwise. It may be remarked that the slight difference noted by Reuter & Sondheimer (1948), between their formulation of the anomalous skin effect in metals at high frequencies and low temperatures and Pippard's (1947) formulation, consists in the absence of a $\cos^2 \theta$ term from the latter, and is due to the use of an expression of type (3) instead of type (5) by Pippard.

4. Equation (4) corresponds to the equation

$$n(\mathbf{r}, \mathbf{v}) = \frac{eE_z \tau}{m} \frac{\partial N_0}{\partial v_z} [1 - \exp \{-(\mathbf{r} - \mathbf{r}_0)/\tau \mathbf{v}\}] \quad [(\mathbf{r} - \mathbf{r}_0) \parallel \mathbf{v}],$$

which is a particular solution of the Boltzmann equation

$$\mathbf{v} \cdot \frac{\partial n}{\partial \mathbf{r}} - \frac{eE_z}{m} \frac{\partial N_0}{\partial v_z} = -\frac{n}{\tau},$$

if $\frac{\partial}{\partial \mathbf{r}} \cdot \left(\frac{eE_z}{m} \frac{\partial N_0}{\partial v_z} \right) = 0$.

This is not, of course, the general solution of the Boltzmann equation; though it may be generalized to include the case $\epsilon \neq 0$, or to include the presence of a longitudinal magnetic field, the solution for a transverse magnetic field is not of this form—in fact, for a transverse field the kinetic theory equation (4) also has to be abandoned and a new approach adopted (§18). In this case the kinetic theory approach does become less easy to apply than the Boltzmann equation approach, though it can still shed useful light on the physical basis of the results obtained by the latter method.

5. We may at once write down the expression for the conductivity of a thin conductor by integrating (5) over the cross-sectional area s :

$$\sigma = \frac{e^2 \tau}{m} \int_0^\infty v^3 \frac{\partial N_0}{\partial v} dv \int_s ds \int_0^{2\pi} d\phi \int_0^\pi d\theta \sin \theta \cos^2 \theta (1 - e^{-OP/l})/s,$$

and if σ_0 is the bulk conductivity,

$$\sigma_0 = \frac{4\pi e^2 \tau}{3 m} \int_0^\infty v^3 \frac{\partial N_0}{\partial v} dv,$$

so that

$$\begin{aligned}\frac{\sigma}{\sigma_0} &= \frac{3}{4\pi s} \int_s ds \int_0^{2\pi} d\phi \int_0^\pi d\theta \sin \theta \cos^2 \theta (1 - e^{-OP/l}) \\ &= 1 - \frac{3}{4\pi s} \int_s ds \int_0^{2\pi} d\phi \int_0^\pi d\theta \sin \theta \cos^2 \theta e^{-OP/l}.\end{aligned}\quad (6)$$

To find the value of σ/σ_0 for any shape of conductor it is merely necessary to express OP in terms of θ , ϕ and the position of the point O , and carry out the integrations. For a thin film or a thin wire, for instance, expressions are immediately obtained identical with those eventually found by Fuchs (1938, equation (17)) and Dingle (1950, equation (10.8)) by integration of the Boltzmann equation.

The case $H = 0, \epsilon \neq 0$

6. In the case $\epsilon \neq 0$ equation (1) has to be replaced by a slightly more complicated equation. For a thin film or a thin wire of circular cross-section (though not for arbitrary cross-section) it is easily seen that before travelling the distance OP , those electrons which have suffered repeated specular reflexions will have traversed equal distances PP' between successive reflexions from the wall, where PP' passes through O , is parallel to OP , and intersects the walls of the metal at P and P' . Letting $OP = a, PP' = b$, we find for the resultant mean free path

$$\begin{aligned}l_1 &= \int_0^a \frac{x}{l} e^{-x/l} dx + (1 - \epsilon) a e^{-a/l} + \epsilon \int_a^{a+b} \frac{x}{l} e^{-x/l} dx + \epsilon(1 - \epsilon)(a + b) e^{-(a+b)/l} \dots \\ &= l[1 - (1 - \epsilon)e^{-OP/l}/(1 - \epsilon e^{-PP'/l})],\end{aligned}\quad (7)$$

and equation (6) becomes

$$\frac{\sigma}{\sigma_0} = \frac{3}{4\pi s} \int_s ds \int_0^{2\pi} d\phi \int_0^\pi d\theta \sin \theta \cos^2 \theta [1 - (1 - \epsilon)e^{-OP/l}/(1 - \epsilon e^{-PP'/l})], \quad (8)$$

which, again, at once leads for a thin film or a thin wire to expressions identical with Fuchs's equation (21) and Dingle's equation (16.2) respectively. By expanding the denominators of these equations and comparing with the equations for $\epsilon = 0$, it may easily be shown that the following simple expression holds for both a thin wire and a thin film:

$$\left(\frac{\sigma}{\sigma_0}\right)_{\epsilon, \kappa} = (1 - \epsilon)^2 \sum_1^\infty \left(n \epsilon^{n-1} \left(\frac{\sigma}{\sigma_0}\right)_{\epsilon=0, n\kappa} \right), \quad (9)$$

which for a thin film may be verified by comparing Fuchs's equations (18) and (22). Here $\kappa = t/l$, where t is the thickness of the film or the diameter of the wire. It should be remarked that Fuchs's approximation (23) for small κ is incorrect; the correct expression is given in appendix 1 below.

The case $H \neq 0$. Longitudinal field

7. On the kinetic theory approach the case of a longitudinal magnetic field ($H \parallel E$) is easier to treat than the case of a transverse field, because in the first case the Lorentz force

$$\mathbf{F} = e(\mathbf{E} + \mathbf{v} \times \mathbf{H}/c) \quad (10)$$

splits up into two independent forces eE_z along the z axis and $e(\mathbf{v} \times \mathbf{H}_z/c)$ which is always perpendicular to the z axis. We can then regard the electric field alone as producing a drift current in the normal way, and the magnetic field simply as modifying the electronic trajectories. When the electric and magnetic fields are not parallel, this approach has to be abandoned; this case is discussed briefly below (§18). For a longitudinal field and for $\epsilon = 0$, the equations (4), (5) and (6) are immediately applicable, where now OP is taken to be the distance from the point O to the point on the surface P along the trajectory of the electrons.

8. The problem of finding the conductivity in the presence of a magnetic field therefore reduces to the solution of equation (6). If the velocity of the electrons at the top of the Fermi distribution is v , then with a magnetic field H along the z axis, electrons travelling at an angle θ to the z axis will move in helical paths of which the projections on the (x, y) plane are circles of radius

$$r = \frac{mv}{eH} \sin \theta = r_0 \sin \theta. \quad (11)$$

It should be noted that the value of r , and hence the effect of the field H , is independent of the direction of H , i.e. whether it is parallel or anti-parallel to E . If now, while the electron is travelling from P to O , its projection on the (x, y) plane traverses an angle ψ around such a circle, then the projection of the distance PO on the (x, y) plane is $\psi r_0 \sin \theta$, and the actual distance PO will be $\sqrt{\psi^2 r_0^2 + l^2}$. Writing $l/r_0 = \eta$, therefore, equations (4) and (6) become

$$n = \frac{eE_z \tau}{m} \frac{\partial N_0}{\partial v_z} [1 - e^{-\psi/\eta}] \quad (12)$$

and

$$\frac{\sigma}{\sigma_0} = 1 - \frac{3}{4\pi s} \int_s ds \int_0^{2\pi} d\phi \int_0^\pi d\theta \cos^2 \theta \sin \theta e^{-\psi/\eta}, \quad (13)$$

where $\psi = \psi(x, y, \theta, \phi)$. The evaluation of this for a thin wire is discussed below

In confirmation of equation (12), Dingle (unpublished) has found by direct integration of the Boltzmann equation for this case

$$n = \frac{eE_z \tau}{m} \frac{\partial N_0}{\partial v_z} \left[1 - \exp - \frac{1}{\eta} \left\{ \sin^{-1} \frac{\alpha r v_r}{[(v_r^2 + v_\theta^2)(v_r^2 + v_\theta^2 + 2\alpha r v_\theta + \frac{1}{2}\alpha r)^{\frac{1}{2}}]} \right. \right. \\ \left. \left. + \sin^{-1} \frac{\alpha [a^2(v_r^2 + v_\theta^2) - (rv_\theta - \frac{1}{2}\alpha \sqrt{a^2 - r^2})^2]^{\frac{1}{2}}}{[(v_r^2 + v_\theta^2)(v_r^2 + v_\theta^2 + 2\alpha r v_\theta + \frac{1}{2}\alpha r)^{\frac{1}{2}}} \right\} \right], \quad (12a)$$

where $\alpha = eH/mc$, r is the distance of the point considered from the axis of the wire, and (v_r, v_θ, v_z) are components of velocity. It may be shown by a certain amount of trigonometry that the term $\{\}$ = ψ . This example shows rather clearly the advantage in clarity of the kinetic theory method.

Evaluation of equation (13) for a thin wire

9. The analytical solution of equation (13) is discussed in appendix 2: an explicit solution is possible only for large fields, and in general one must resort to numerical or graphical methods. By careful choice of procedure it is possible to obtain reasonably

accurate and detailed results without undue labour; the steps involved are described briefly below. As in the treatment of a thin wire in the absence of magnetic field, it is advantageous to integrate first over all electrons having the same value of ϕ , i.e. travelling in the same direction at the instant considered; the integral then becomes independent of ϕ by symmetry, and we may rewrite (13) in the form

$$\frac{\sigma}{\sigma_0} = \frac{3}{s} \int_0^{\frac{1}{2}\pi} d\theta \cos^2 \theta \sin \theta \int_s ds (1 - e^{-\psi/\eta})_\phi. \quad (14)$$

Now those electrons which, since colliding with the wall, have turned through angles between ψ and $\psi + d\psi$ and are, at the instant considered, travelling in the direction ϕ , θ will be located in a strip, of area $s(\psi) d\psi$ say, within the total cross-sectional area. If we denote the proportion of the total cross-section occupied by these electrons by $p(\psi) d\psi$, we may rewrite (14) as

$$\frac{\sigma}{\sigma_0} = 3 \int_0^{\frac{1}{2}\pi} d\theta \sin \theta \cos^2 \theta \int_0^\infty p(\psi) (1 - e^{-\psi/\eta}) d\psi, \quad (15)$$

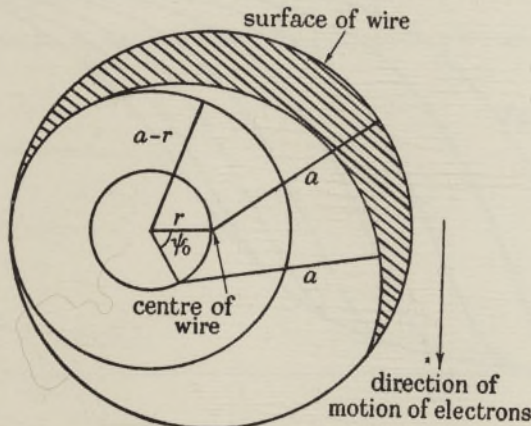


FIGURE 1. Construction for the determination of $P(\psi_0)$.

where ψ ranges between 0 and 2π for those electrons which can hit the wall at some point in their trajectory, and $\psi = \infty$ for those electrons which (in a strong enough field) can never hit the wall. Since for these $e^{-\psi/\eta} = 0$, we have

$$\frac{\sigma}{\sigma_0} = 3 \int_0^{\frac{1}{2}\pi} d\theta \sin \theta \cos^2 \theta \left[1 - \int_0^{2\pi} p(\psi) e^{-\psi/\eta} d\psi \right]. \quad (16)$$

Now $p(\psi)$ is a function only of the ratio of the radius of the wire, a , to the radius of the projection of the orbit, $r = r_0 \sin \theta$, i.e. of the ratio $2 \sin \theta / \eta \kappa$, where $\kappa = 2a/l$.

Geometrically, it is easier to find $P(\psi_0) = \int_0^{\psi_0} p(\psi) d\psi$ than to find $p(\psi)$ itself. Figure 1 shows the construction for the example $r/a = 2 \sin \theta / \eta \kappa = 0.3$, and $\psi_0 = 60^\circ$. If, at the instant considered, all electrons are travelling in the direction shown by the arrow, then the shaded area will contain all those which have turned through angles $\psi \leq \psi_0$, i.e. the area shaded is a measure of $P(\psi_0)$. The electrons within the circle of radius $(a-r)$ are those for which $\psi = \infty$. In this way $P(\psi_0)$ was evaluated for eight

values of r/a between 0.1 and 10. Now by partial integration, we may express the integral $\int_0^{2\pi} p(\psi) e^{-\psi/\eta} d\psi$ of equation (16) in terms of $P(\psi_0)$; we have

$$\int_0^{2\pi} p(\psi) e^{-\psi/\eta} d\psi = P(2\pi) e^{-2\pi/\eta} + \frac{1}{\eta} \int_0^{2\pi} P(\psi) e^{-\psi/\eta} d\psi. \quad (17)$$

Hence the values of $\int_0^{2\pi} p(\psi) e^{-\psi/\eta} d\psi$ were found, for the values of r/a considered, for values of η between 0.2 and 200. Denoting

$$1 - \int_0^{2\pi} p(\psi) e^{-\psi/\eta} d\psi \quad \text{by} \quad S_1(r/a, \eta) = S_1(2 \sin \theta / \eta \kappa, \eta) = S_1(\sin \theta / \kappa, \eta),$$

it was then possible to plot S_1 against $\kappa / \sin \theta$ for various values of η , as shown in figure 2. Finally, since $\sigma / \sigma_0 = \int_0^1 S_1 d(\cos^3 \theta)$, the values of σ / σ_0 for given κ and

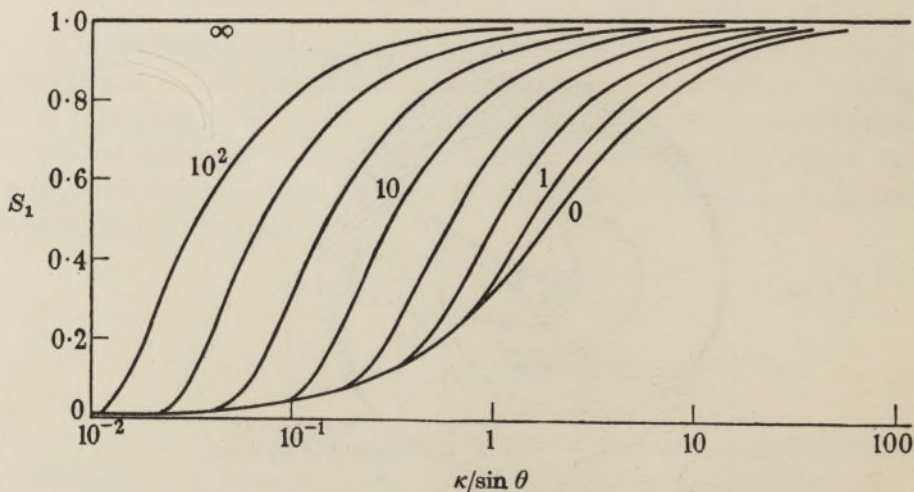


FIGURE 2. S_1 against $\kappa / \sin \theta$ for different values of $\frac{1}{\eta}$.

η could be found by re-plotting S_1 against $\cos^3 \theta$, as in figure 3, plotted for $\kappa = 0.1$, $\eta = 0$ and $\eta = 20$, and integrating again. In this way σ / σ_0 was found for values of η between 0.2 and 200, and values of κ between 0.01 and 10. All integrations were performed graphically, with the aid of a planimeter. As a check on the accuracy, σ / σ_0 was at the same time evaluated by a very similar method for $\eta = 0$, i.e. zero magnetic field, and the results compared with the accurately known values (Dingle 1950).

10. The values found for σ / σ_0 are given in table 1. Here the values for $\eta = 0$ are those given by Dingle, and the values for $\eta \kappa \geq 5$ are those obtained from equation (A.6) of appendix 2. The values given for the range $0 < \eta \kappa < 5$ are those obtained graphically as described above. Graphical solutions were also obtained for $\eta = 0$ and for $\eta \kappa \geq 5$; by comparison of the values so obtained with the exact values, and also by independent consideration of the inaccuracies involved, it is estimated that the values obtained graphically are probably not in error by more than 0.5 % for

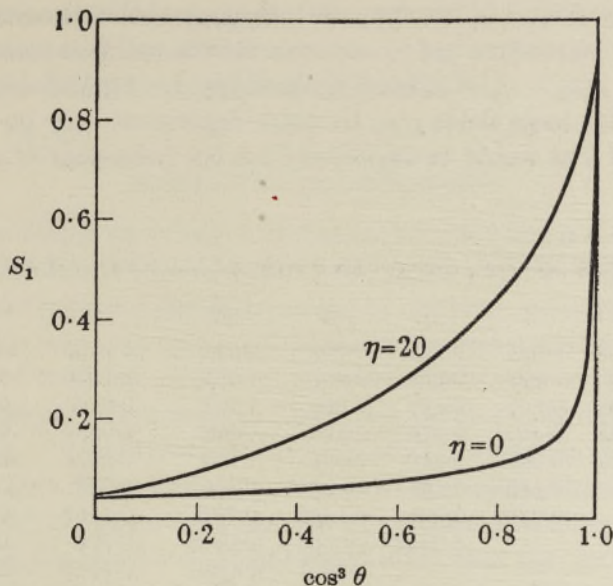


FIGURE 3. S_1 against $\cos^3 \theta$, for $\kappa = 0.1$, for $\eta = 0$ and $\eta = 20$.

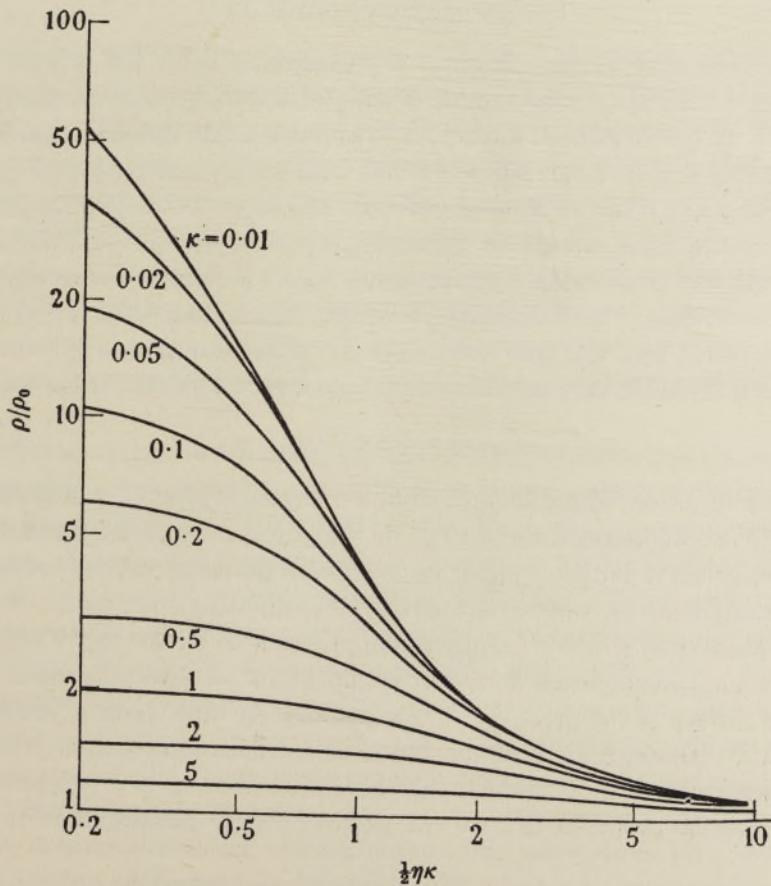


FIGURE 4. ρ/ρ_0 against $\frac{1}{2}\eta\kappa$, for various κ .

$\sigma/\sigma_0 \geq 0.5$, and more than 1 % for $\sigma/\sigma_0 \geq 0.1$; they are rather less accurate at smaller values, but seldom more than $\pm 3\%$ out even for the smallest values.

Figure 4 shows $\rho/\rho_0 = \sigma_0/\sigma$ plotted against $\frac{1}{2}\eta\kappa$, i.e. against $a/r_0 = eaH/mvc$. It will be seen that for large fields ρ/ρ_0 becomes dependent only on the product $\eta\kappa$, i.e. independent of l , as would be expected from the behaviour of equation (16) for large η .

TABLE I. VALUES OF σ/σ_0 OBTAINED FROM EVALUATION OF EQUATION (13).

$\kappa \frac{1}{2}\eta$	0	10^{-4}	1	10^1	10^2	10	10^4	10^6	10^8
10	0.925	0.933	0.946	0.963	0.979	0.989	0.9948	0.9975	0.9988
5	0.853	0.869	0.893	0.928	0.959	0.979	0.9896	0.9950	0.9977
2	0.678	0.693	0.748	0.826	0.899	0.947	0.9741	0.9876	0.9942
1	0.489	0.504	0.555	0.674	0.805	0.896	0.9484	0.9753	0.9884
0.5	0.318	0.324	0.340	0.440	0.635	0.799	0.8984	0.9509	0.9768
0.2	0.158	—	0.163	0.186	0.295	0.549	0.758	0.8801	0.9425
0.1	0.0873	—	0.0899	0.0960	0.1266	0.272	0.5565	0.7691	0.8872
0.05	0.0464	—	—	0.0482	0.0556	0.0968	0.272	0.5746	0.7821
0.02	0.0192	—	—	—	0.0201	0.0281	0.0612	0.1992	0.5140
0.01	0.00976	—	—	—	—	0.0109	0.0200	0.0598	0.228

INTERPOLATION FORMULAE

11. For a thin wire in the absence of a magnetic field, the simple Nordheim expression $\sigma_0/\sigma \approx 1 + 1/\kappa$ yields values of σ/σ_0 remarkably close to the true values (Dingle 1950). In the Nordheim theory, the resultant mean free path l_T is found from the equation $1/l_T = 1/l + 1/l_W$, where l is the bulk mean free path and l_W the mean distance to the walls. This is erroneous because the form of equation implies additive scattering probabilities, which in turn implies that the probability of making a collision with the wall varies exponentially with the distance travelled, which is untrue. Nevertheless, the differences between the values of σ/σ_0 given by the Nordheim equation and the true values are never greater than 5 % over the whole range of κ . This makes it very useful as an interpolation formula, when written in the form

$$\rho/\rho_0 = 1 + \alpha(\kappa)/\kappa, \quad (18)$$

where $\alpha(\kappa)$ is a function, found from the known values of $\rho/\rho_0(\kappa)$, which varies slowly from 1 to 0.75 as κ increases from 0 to ∞ . It was by the use of this function that the values of σ/σ_0 given in Dingle's paper for $\epsilon = \frac{1}{2}$ and for intermediate values of κ were found, using equation (9) above; this involved evaluating σ/σ_0 for $\epsilon = 0$ for a large number of values of κ , which was only made practicable by the use of equation (18). A similar simple interpolation function would be of considerable value in supplementing the values given in table 1. An attempt to find such a function by an adaptation of Nordheim's method was, however, unsuccessful; the resulting formulae were cumbersome and not particularly accurate. For $\eta\kappa \geq 2$, equation (A6) of appendix 2 may be used; for $\eta\kappa \geq 10$ this equation may be simplified to

$$\frac{\sigma}{\sigma_0} \approx 1 - \frac{3}{4\kappa(1 + \eta^2/4)} \left[1 + \frac{\eta^2}{8} (1 - e^{-2\pi/\eta}) \right] \quad (19)$$

with sufficient accuracy. Unfortunately, the region of large $\eta\kappa$ is the least interesting from the experimental point of view; it appears impossible to devise a simple and accurate formula valid in the important region $\eta\kappa \sim 1$.

APPLICATION TO EXPERIMENT

12. One of the major advantages of measurements using a magnetic field, compared with measurements made in zero field, is that all the required information may be obtained from one specimen only, by making measurements at various temperatures. This is in principle possible also with measurements in zero field, but only if the form of variation of σ_0 with temperature is accurately known. Since σ_0 cannot be measured on the specimen itself, this involves the doubtful assumption that the form of $\sigma_0(T)$, and therefore the form of $l(T)$, where l is the 'bulk' mean free path, is the same for a thin specimen as for a bulk specimen. Alternatively, σ may be measured at one temperature for a number of specimens of different diameter; this involves, however, the equally doubtful assumption that the 'bulk' mean free path is the same for all specimens, and that no variation in residual resistivity occurs between the specimens. It is probably some such variation which accounts for the rather large scatter of Andrew's (1949) observations about the theoretical curves (cf. Dingle 1950).

13. If we plot, not ρ/ρ_0 against $\frac{1}{2}\eta\kappa$ as in figure 4, but $\kappa\rho/\rho_0$ against $\frac{1}{2}\eta\kappa$, both the ordinates and abscissae become proportional to directly measurable quantities. We have $\kappa\rho/\rho_0 = 2ap/\rho_0 l$, and since $\rho_0 l$ is independent of temperature, we may write this $\rho/\rho_0(l = 2a)$, the ratio of the observed resistivity at any temperature to the bulk resistivity at a temperature such that $l = 2a$. Also $\eta\kappa/2 = a/r_0 = (ea/mvc)H$, and is directly proportional to the applied magnetic field. If, therefore, we plot the observed values of ρ against H at a number of temperatures, on logarithmic scales, we shall obtain a family of curves which should be directly superposable on the theoretical curves of $\kappa\rho/\rho_0$ against $\eta\kappa/2$, and the proportionality constants between the two sets of curves will give $\rho_0(l = 2a)$ and hence l , and (ea/mvc) and hence mv , directly.

14. In setting up and evaluating equation (13), we have tacitly made several assumptions which require further consideration before we can confidently compare the results with measurements on actual metals. First, we have assumed throughout that $\epsilon = 0$, i.e. that all electrons are diffusely reflected at the surface. Extension of the theory to $\epsilon \neq 0$ would be very laborious: equation (7) depends on symmetry considerations which are no longer applicable in the presence of a magnetic field, and it is unlikely that the simple result of equation (9) will still be valid. Moreover, the introduction of a third parameter ϵ besides κ and η , varying in an unknown way with temperature, would make it impossible to draw unique conclusions from the experimental results. For both these reasons, therefore, it is fortunate that independent evidence strongly indicates that $\epsilon = 0$ at all temperatures. This evidence comes from measurements by the author on the anomalous skin effect at high frequencies and low temperatures, where the mean free path becomes long compared with the classically predicted skin depth. The theory of the effect has been worked

out by Pippard (1947) and by Reuter & Sondheimer (1948) for the cases $p = 0$ and $p = 1$, where p is a parameter comparable with our ϵ . It has been found (Chambers 1950) that the observed behaviour of several metals agrees very closely with the $p = 0$ curve, and cannot be fitted to the $p = 1$ curve. It has been pointed out by Pippard that in the anomalous skin effect the current is carried almost entirely by electrons travelling at very small angles to the surface, and hence the value of p is presumably determined chiefly by the behaviour of these electrons on reflexion. If specular reflexion occurs at all, it seems most likely to occur for these electrons, travelling at small angles to the surface, and since it is not observed for them, i.e. since $p = 0$, it seems reasonable to expect that $\epsilon = 0$ also for the d.c. case, where electrons travelling at all angles to the surface are involved.

15. Secondly, we have assumed the validity of the classical kinetic theory or Boltzmann theory approach; that is to say, we have neglected quantization effects. Jones & Zener (1934) and Wilson (1936, p. 168) have pointed out that the Boltzmann equation ceases to be strictly applicable for $r_0 \leq l$, i.e. for $\eta \geq 1$ in our notation. However, it is usually assumed that quantization effects will not greatly alter the behaviour of the system unless the field is rather higher than those envisaged here.

16. Lastly, and most important, we have assumed a free-electron model, and we have assumed the existence of an isotropic mean path. It need hardly be said that these are both gross over-simplifications for any but group I metals; nevertheless, it might be expected that for more complex metals the experimental results would be of the same general form, and that from them some information about electronic mean free paths and momenta could be obtained. In one respect, however, the free-electron model predicts behaviour from which that of real metals departs strongly: it gives no bulk magneto-resistance effect, or at any rate an extremely small one. In fact, as Peierls (1931) first pointed out, bulk magneto-resistance effects are due entirely to the deviations of real metals from the free-electron model. This is confirmed by the experimental observations: the effect is very small in sodium, which most closely approximates to the free-electron model, and becomes progressively greater for less 'perfect' metals. Unfortunately, the effect is strongly temperature-dependent, becoming greater at low temperatures; in fact the relative change of resistance $\Delta\rho/\rho_0$ is approximately the same function of the ratio H/ρ_0 at all temperatures, so that as ρ_0 falls, the same relative increase in resistance will be brought about by a proportionately smaller field. (See, for example, Gruneisen (1945) for a review of the subject.) Thus the method described in §13 to measure the mean free path and electron momentum can only be used for metals for which the bulk magneto-resistance effect is not too large; otherwise the increase of resistance with field due to this cause will swamp the decrease predicted for thin specimens by the free-electron theory. By comparison of the experimental data on the bulk effect with the expected behaviour of thin specimens, it appears that application of the method will probably only be possible for 'good' metals such as the group I metals, and perhaps not for all of them. Dr MacDonald has informed me that in measurements on thin films of gold, silver and tin, the bulk magneto-resistance effect was found to swamp the expected decrease in resistance in each case.

COMPARISON WITH EXPERIMENT

17. Through the kindness of Dr MacDonald, who lent me one of his specimens of sodium wire, 30μ in diameter, I have recently been able to make some experimental observations with which to compare the theoretical results given above. The specimen was placed in a cryostat capable of being heated electrically above the bath temperature, and the magnetic field was provided by a water-cooled solenoid capable of giving fields up to about 8000 gauss, uniform to within 1 or 2 % over the volume occupied by the specimen. The R - H curves obtained at various temperatures are

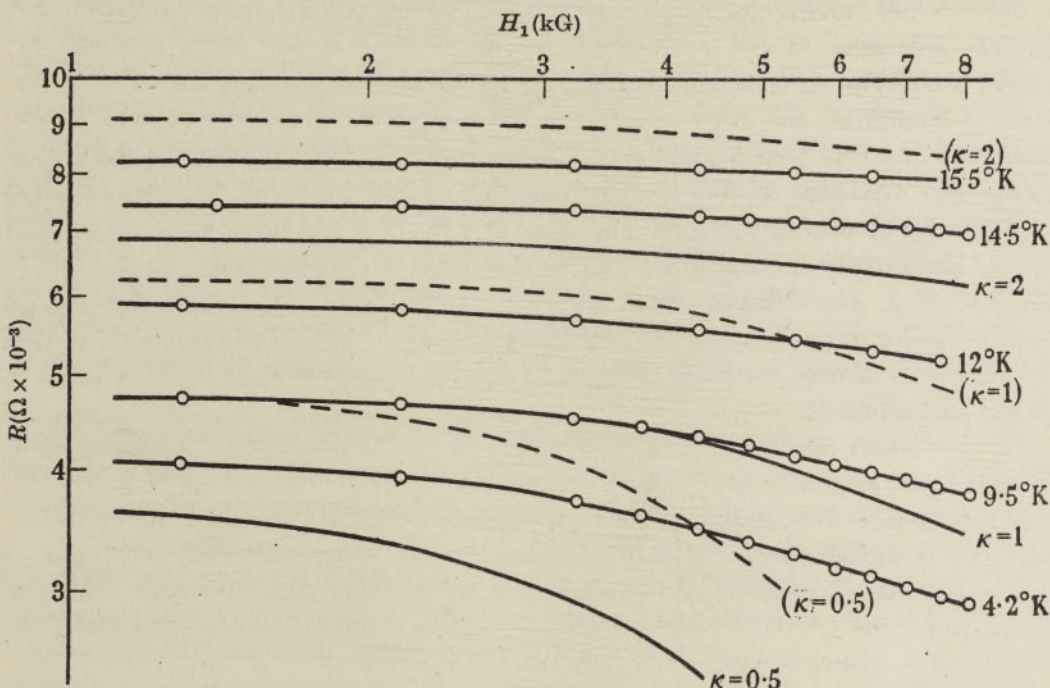


FIGURE 5. Experimental results on 30μ sodium wire, with theoretical curves.

shown in figure 5, and also shown are the theoretical curves for $\kappa = 0.5$, 1 and 2, adjusted to fit as well as possible. The departure from theory in high fields is presumably due to the bulk magneto-resistance effect discussed above. The magnitude of the departure is in good agreement with that expected from Justi's (1948) measurements on the bulk magneto-resistance effect in sodium. From the fit of the theoretical and experimental results, values for σ/l and for v of $9.0 \times 10^{10} \text{ ohm}^{-1} \text{ cm.}^{-2}$ and $1.0 \times 10^8 \text{ cm./sec.}$ are obtained, as described in § 13, which agree reasonably well with the values predicted by the free-electron theory, of $7.0 \times 10^{10} \text{ ohm}^{-1} \text{ cm.}^{-2}$ and $1.07 \times 10^8 \text{ cm./sec.}$ respectively.

The discrepancy between the theoretical and observed values of σ/l , however, appears to be real; the theoretical curves obtained assuming $\sigma/l = 7.0 \times 10^{10} \text{ ohm}^{-1} \text{ cm.}^{-2}$ are shown dotted in figure 5, and it will be seen that the discrepancies are too great to be accounted for by the bulk magneto-resistance effect.

TRANSVERSE FIELD

18. In conclusion, we may consider briefly the applicability of the kinetic theory method to transverse field problems. The equations of motion of a free electron subjected to electric and magnetic fields E_z and H_x are

$$\left. \begin{aligned} v_z &= v_0 \sin \left(\frac{eH_x}{mc} t + \delta \right), \\ v_y &= -v_0 \cos \left(\frac{eH_x}{mc} t + \delta \right) + \frac{cE_z}{H_x}, \end{aligned} \right\} \quad (20)$$

so that a freely moving electron acquires no mean drift velocity in the z direction, but simply 'precesses' in the y direction. If the electron is not freely moving, but suffers a collision after a time t , there will in general result currents in both the y and z directions; the mean current in the y direction is reduced to zero by the setting up of a Hall field E_y , and under these conditions the conductivity is given by \bar{J}_z/E_s . The existence of the Hall field greatly complicates the solution of these problems by kinetic methods for thin films and wires, particularly since, as pointed out by MacDonald & Sarginson, we can in general no longer assume E_y to be independent of y . In addition, the evaluation of the results for a case of such low symmetry as a thin wire in a transverse magnetic field would be extremely laborious; the relatively simple methods used in § 9 for the longitudinal field case would no longer be applicable.

The particular case treated by Sondheimer can, however, be treated fairly simply, though not so elegantly as on the Boltzmann theory approach, and since in this case it is not obvious from simple physical arguments how the presence of the magnetic field affects the conductivity at all, we shall indicate briefly how this arises.

19. The case considered by Sondheimer is that of a thin film with an electric field E_z applied in the z direction and a magnetic field H_x perpendicular to the plane of the film. It is in this case possible to simplify the problem, since the Hall field is independent of position (the film being effectively of infinite extension in the (y, z) plane) by putting $E_y = 0$ and regarding E_z as the resultant of the applied field and the Hall field. Both \bar{J}_z and \bar{J}_y will then be non-zero; if the resultant total current is \bar{J} , then the component of E_z in the direction of \bar{J} is to be regarded as the applied field, and the perpendicular component as the Hall field. Equations (20) then give the velocities v_y and v_z at time t of an electron following a path such that at time $t = 0$ it passes through a given point O in the metal with velocities

$$\left. \begin{aligned} v_z(0) &= v_0 \sin \delta, \\ v_y(0) &= -v_0 \cos \delta + \frac{cE_z}{H_x}. \end{aligned} \right\} \quad (21)$$

The velocity v_x of the electron in the x direction (across the film) is independent of time. Then if

$$v = [v_x^2 + v_y(0)^2 + v_z(0)^2]^{\frac{1}{2}}$$

is the speed of the electron at time $t = 0$, at time t its speed will, assuming $cE_z/H_x \ll v$, be given by

$$\Delta v_t = v_t - v = -\frac{v_0 c}{v} \frac{E_z}{H_x} \left[\cos \left(\frac{eH_x}{mc} t + \delta \right) - \cos \delta \right] \quad (22)$$

The excess number density of electrons having speed v_t , compared with those having speed v , is $(\partial N_0 / \partial v) \Delta v_t = \delta n_t$ say, and these have a probability $e^{t/r}$ of reaching point O (t being negative).

Hence the excess number density of electrons travelling through point O with velocity components $v_x, v_y(0), v_z(0)$ is given by

$$n(0) = \int_{-T}^0 \frac{\partial}{\partial t} (\delta n_t) e^{t/r} dt = \frac{\partial N_0}{\partial v} \int_{-T}^0 \frac{\partial \Delta v_t}{\partial t} e^{t/r} dt, \quad (23)$$

where the limit of integration, $-T$, corresponds to electrons which have travelled from points at the surface of the metal. Using (22) and writing $t = x/v \cos \theta$, $T = x_0/v \cos \theta$, $r = mvc/eH_x$, $\tau = l/v$, we obtain from equation (23)

$$n(0) = \frac{\partial N_0}{\partial v} \frac{eE_z v_0}{mvv_x} \int_{-x_0}^0 \sin [(x/r \cos \theta) + \delta] e^{x/l \cos \theta} dx, \quad (24)$$

and on integrating this it becomes identical with the value of $n(0)$ given by Sondheimer, putting $E_y = 0$. The present solution makes clear the physical origin of the oscillations in conductivity found by Sondheimer. The oscillations in speed given by (22) give rise to oscillations in the excess number density at the points from which the electrons come which pass through the point O , the contribution to the current at O of electrons which have travelled freely from a point distance x away being given by the integrand of (24). It is clear that if l is large compared with x , and x is of the same order as r , the current density may fluctuate with the ratio x/r , as found by Sondheimer.

I should like to thank Dr MacDonald for the loan of the specimen of sodium wire on which the experimental measurements were made, and Dr MacDonald, Miss Sarginson, Dr Sondheimer and Mr Dingle for helpful discussions and for showing me their results before publication.

APPENDIX 1. *Explicit solution for thin films in zero magnetic field*

By the use of the approximation

$$\int_{\kappa}^{\infty} \frac{e^{-x}}{x} dx \approx \ln 1/\kappa - c + 0.9755\kappa$$

(where c is Euler's constant), valid to $< 0.5\%$ for $\kappa < 0.2$, Fuchs's expression (18) for σ/σ_0 with $\epsilon = 0$ may be reduced to

$$\left(\frac{\sigma}{\sigma_0}\right)_{\epsilon=0, \kappa} \approx \frac{3\kappa}{4} [\ln 1/\kappa + 0.4228] + 0.4816\kappa^2 \dots, \quad (A 1)$$

valid to $< 1\%$ for $\kappa < 0.2$. Substituting this in equation (9), § 6, we obtain for $\epsilon \neq 0$

$$\left(\frac{\sigma}{\sigma_0}\right)_{\epsilon, \kappa} \approx \frac{1+\epsilon}{1-\epsilon} \left(\frac{\sigma}{\sigma_0}\right)_{\epsilon=0, \kappa} + \frac{4\epsilon}{(1-\epsilon)^2} 0.4816\kappa^2 - \frac{3\kappa}{4} (1-\epsilon)^2 \sum_1^{\infty} n^2 \epsilon^{n-1} \ln n. \quad (A 2)$$

This expression is applicable provided that the terms in the summation (9) for which $n\kappa \geq 0.2$ are small compared with those for which $n\kappa < 0.2$. For $\epsilon = \frac{1}{2}$, this restricts

its application to values of κ less than about 0.02, and for $\epsilon = \frac{9}{10}$, less than about 0.004. The term $\sum_1^{\infty} n^2 e^{n-1} \ln n$ in (A 2) is equal to 15.48 for $\epsilon = \frac{1}{2}$, and 6060 for $\epsilon = \frac{9}{10}$.

This expression gives values of $(\sigma/\sigma_0)_{\epsilon, \kappa}$ somewhat greater than those given by Fuchs's equation (23) (in which $1-\epsilon$ is presumably a misprint for $(1-\epsilon)^{-1}$) and plotted in his figure 2, but the difference does not materially affect his interpretation of Lovell's experimental results.

APPENDIX 2. Analytical solution of equation (13)

1. The analytical approach to the solution of equation (13) is identical with the graphical approach of § 9, and the same notation will be used. Let the ratio $r/a = \gamma$. Then by consideration of figure 1, and the corresponding figure for $\gamma > 1$, it is readily shown that for $\gamma \leq 1$,

$$\pi p(\psi) = \gamma(1-\gamma) + \gamma^2 \cos^2 \frac{1}{2}\psi + \gamma \cos \frac{1}{2}\psi (1 - \gamma^2 \sin^2 \frac{1}{2}\psi)^{\frac{1}{2}} \quad (0 \leq \psi \leq 2\pi) \quad (\text{A } 3)$$

and for $\gamma \geq 1$,

$$\begin{aligned} \pi p(\psi) &= 2\gamma \cos \frac{1}{2}\psi (1 - \gamma^2 \sin^2 \frac{1}{2}\psi)^{\frac{1}{2}} \quad (0 \leq \psi \leq 2\sin^{-1}(1/\gamma)) \\ &= 0 \quad (2\sin^{-1}(1/\gamma) < \psi \leq 2\pi). \end{aligned} \quad (\text{A } 4)$$

2. Now for $\eta\kappa \geq 2$, $\gamma = r/a = 2\sin\theta/\eta\kappa$ remains less than 1 for all values of θ , while for $\eta\kappa < 2$, we have $\gamma < 1$ for small θ and $\gamma > 1$ for large θ ($\sim \frac{1}{2}\pi$). Physically, this means simply that for strong enough fields ($\eta\kappa \geq 2$) all electronic trajectories are curved into paths of radius less than the wire radius; for smaller fields, those electrons travelling at small angles to the axis and therefore having small transverse velocities will still follow such paths, but electrons moving at greater angles to the axis will follow paths of radius greater than the wire radius. Solution for $\eta\kappa < 2$ is therefore much more difficult than for $\eta\kappa \geq 2$, and will only be considered briefly.

3. The value of $S_1 = 1 - \int_0^{2\pi} p(\psi) e^{-\psi/\eta} d\psi$ may be found by expanding the root $(1 - \gamma^2 \sin^2 \frac{1}{2}\psi)^{\frac{1}{2}}$ in (A 3) and (A 4). For $\gamma < 1$, the series solution converges rapidly; taking

$$(1 - \gamma^2 \sin^2 \frac{1}{2}\psi)^{\frac{1}{2}} \approx 1 - \frac{1}{2}\gamma^2 + \frac{1}{2}\gamma^2 \cos^2 \frac{1}{2}\psi,$$

we obtain

$$\begin{aligned} \pi(1 - S_1) &\approx \gamma \left[\frac{2}{\alpha} (1 - e^{-\pi\alpha}) + \frac{2\alpha}{\alpha^2 + 1} (1 + e^{-\pi\alpha}) \right] + \gamma^2 \left[\frac{\alpha}{\alpha^2 + 4} - \frac{1}{\alpha} \right] (1 - e^{-\pi\alpha}) \\ &\quad + \frac{1}{4} \gamma^3 \left[\frac{\alpha}{\alpha^2 + 9} - \frac{\alpha}{\alpha^2 + 1} \right] (1 + e^{-\pi\alpha}) \end{aligned} \quad (\text{A } 5)$$

where $\alpha = 2/\eta$. Hence, for $\eta\kappa > 2$, so that $\gamma < 1$ for all θ , we have

$$\begin{aligned} \frac{\sigma}{\sigma_0} &= 3 \int_0^{\frac{1}{2}\pi} S_1 \cos^2 \theta \sin \theta d\theta \\ &\approx 1 - \frac{3}{4\kappa(1 + \frac{1}{4}\eta^2)} \left[1 + \frac{\eta^2}{8} (1 - e^{-2\pi/\eta}) \right] + \frac{3}{16\kappa^2} \frac{1}{(1 + \frac{1}{4}\eta^2)(1 + 9\eta^2/4)} (1 + e^{-2\pi/\eta}) \\ &\quad + \frac{4}{5\pi\kappa^2} \frac{\eta}{1 + \eta^2} (1 - e^{-2\pi/\eta}) \end{aligned} \quad (\text{A } 6)$$

This expression was used in deriving the values of σ/σ_0 for $\eta\kappa \geq 5$ given in table 1. The series converges very rapidly; the next two terms, given by the next two terms in the expansion of $(1 - \gamma^2 \sin^2 \frac{1}{2}\psi)^{\frac{1}{2}}$, give a contribution less than

$$\frac{0.1\eta}{1 + \frac{1}{4}\eta^2} [(\eta\kappa)^{-5} + 1.6(\eta\kappa)^{-7}],$$

and are consequently always negligible for $\eta\kappa \geq 5$, and only become important for $\eta\kappa \sim 2$ when $\eta \sim 2$.

4. For $\eta\kappa < 2$, an expression for S_1 may still be obtained by expanding the root in (A3) and (A4), but for $\gamma > 1$ the resulting expression converges only slowly, because the value of $(1 - \gamma^2 \sin^2 \frac{1}{2}\psi)^{\frac{1}{2}}$ falls to zero at the upper limit of integration. Moreover, to obtain the value of σ/σ_0 from S_1 it is necessary to evaluate integrals of the form

$$\int_{\sin^{-1}(\frac{1}{2}\eta\kappa)}^{\frac{1}{2}\pi} d\theta \sin^{2n} \theta \exp\{-\alpha \sin^{-1}(\eta\kappa/2 \sin \theta)\}.$$

Integration of this has not been attempted. It may be noted, however, that for very small fields, i.e. $\eta\kappa \rightarrow 0$, where we may replace (A4) by $\pi p(\psi) \approx 2\gamma(1 - \frac{1}{4}\gamma^2\psi^2)^{\frac{1}{2}}$, and where we may take $\gamma > 1$ over the whole range of θ from 0 to $\frac{1}{2}\pi$, the expression for σ/σ_0 reduces to

$$\frac{\sigma}{\sigma_0} \approx 1 - \frac{12}{\pi} \int_0^1 dx (1 - x^2)^{\frac{1}{2}} \int_0^{\frac{1}{2}\pi} d\theta \cos^2 \theta \sin \theta e^{-\kappa x / \sin \theta},$$

where we have put $\gamma\psi = 2x$. This is identical with Dingle's equation (10.8) for a thin wire in the absence of a magnetic field. It would be possible by going to higher approximations to find an explicit solution for σ/σ_0 in very small fields, in terms of the value of σ/σ_0 for $H = 0$, but this could only be valid for $\eta\kappa \leq 0.1$, and reference to table 1 and figure 4 shows that in this region σ/σ_0 changes only very slightly.

REFERENCES

- Andrew, E. R. 1949 *Proc. Phys. Soc.* **62**, 77.
 Chambers, R. G. 1950 *Nature*, **165**, 239.
 Dingle, R. B. 1950 *Proc. Roy. Soc. A*, **201**, 545.
 Eucken, A. & Förster, F. 1934 *Nach. Ges. Wiss. Göttingen*, N.S. **1-2**, 43, 129. See also *Ann. Phys., Lpz.*, **28**, 603 (1937), **33**, 733 (1938) (Riedel); **30**, 494 (1937) (Reuter); **40**, 121 (1941) (Möser).
 Fuchs, K. 1938 *Proc. Camb. Phil. Soc.* **34**, 100.
 Gruneisen, E. 1945 *Ergebn. Exakt. Naturw.* **21**, 50.
 Jones, H. & Zener, C. 1934 *Proc. Roy. Soc. A*, **144**, 101.
 Justi, E. 1948 *Ann. Phys., Lpz.* (6) **3**, 183.
 Lovell, A. C. B. 1936 *Proc. Roy. Soc. A*, **157**, 311.
 Lovell, A. C. B. 1938 *Proc. Roy. Soc. A*, **166**, 270.
 Lovell, A. C. B. & Appleyard, E. T. S. 1937 *Proc. Roy. Soc. A*, **158**, 718. See also Appleyard, E. T. S. & Bristow, J. R. 1939, *Proc. Roy. Soc. A*, **172**, 530.
 MacDonald, D. K. C. 1949 *Nature*, **163**, 639.
 MacDonald, D. K. C. & Sarginson, K. 1949 *Nature*, **164**, 921.
 Nordheim, L. 1934 *Act. Sci. et Ind.* no. 131. Paris: Hermann. See also Planck, W. 1914, *Phys. Z.* **15**, 569; Tisza, L. 1931, *Naturwissenschaften*, **19**, 86; Nordheim, L. 1931, *Ann. Phys., Lpz.*, **9**, 607.

- Peierls, R. 1931 *Ann. Phys., Lpz.*, **10**, 97.
 Pippard, A. B. 1947 *Proc. Roy. Soc. A*, **191**, 385.
 Reinders, W. & Hamburger, L. 1931 *Ann. Phys., Lpz.*, **10**, 649, 789.
 Reuter, G. E. H. & Sondheimer, E. H. 1948 *Nature*, **161**, 394; *Proc. Roy. Soc. A*, **195**, 336.
 Sondheimer, E. H. 1949 *Nature*, **164**, 920.
 Thomson, J. J. 1901 *Proc. Camb. Phil. Soc.* **11**, 120.
 Wilson, A. H. 1936 *Theory of metals*. Cambridge University Press.
-

The structure of linear relativistic wave equations.

II. Representations

By K. J. LE COUTEUR

Department of Theoretical Physics, University of Liverpool

(Communicated by P. A. M. Dirac, F.R.S.—Received 22 February 1950)

A representation of the spin matrices $I_{\mu\nu}$ and of the matrices α_μ , associated with the wave equations of part I, is constructed. In this representation s , the total spin, is diagonal, which simplifies the calculation of the simultaneous mass and spin eigenvalues. Examples of mass-spin spectra are given, and it is proved that in certain, easily recognized, cases the mass eigenvalues are not all independent.

The matrix elements of the magnetic moment are calculated, and an example is given of a particle with an intrinsic magnetic moment equal to that of the proton.

1. INTRODUCTION

In part I (Le Couteur 1950, referred to as I) the discussion of linear relativistic wave equations of finite order was carried as far as possible without use of matrix representations of the α_μ and $I_{\mu\nu}$, which characterize the equations. This paper describes an explicit representation of these matrices.

It was shown in I (§ 6) that the physical properties of the wave equation appear most simply in a representation with α_0 and S , the total spin angular momentum, in diagonal form. Therefore, it is convenient to choose the basis of each representation (p, q) of the $I_{\mu\nu}$ so that S is diagonal as well as p and q ; then the coupling matrices which generate the α_μ can be worked out by the method indicated in § 8 of I. Finally, if desired, α_0 can be brought to diagonal form by a unitary transformation which commutes with S . This procedure differs from that of Dirac (1936) and Bhabha (1945) who expressed the coupling matrices in terms of spinor matrices $U^\alpha(k)$ and $V^\alpha(k)$. In that representation S is not diagonal and a complicated transformation, which has been worked out by Wild (1947), is required to diagonalize it.

The matrix representation of the α_μ directly relates the arbitrary coupling coefficients C_{ab} to the mass-spin spectrum and to the magnetic moment of the particle.